AGU PUBLICATIONS

Water Resources Research

RESEARCH ARTICLE
10.1002/2015WR017752

Dry season streamflow persistence in seasonal climates

David N. Dralle[1], Nathaniel J. Karst[2], and Sally E. Thompson[1]

[1]Department of Civil and Environmental Engineering, University of California, Berkeley, California, USA, [2]Division of Mathematics and Science Division, Babson College, Wellesley, Massachusetts, USA

Key Points:
- Derived probabilistic model for the persistence time of dry season high flow conditions
- Successfully predicts mean, but not variance; attributed to inter-annual recession model variation
- Proposed framework for using crossing statistics (e.g., persistence time) to forecast ecologic risk

Supporting Information:
- Supporting Information S1
- Figure S1
- Figure S2

Correspondence to:
D. N. Dralle,
dralle@berkeley.edu

Citation:
Dralle, D. N., N. J. Karst, and S. E. Thompson (2015), Dry season streamflow persistence in seasonal climates, *Water Resour. Res.*, *51*, doi:10.1002/2015WR017752.

Received 26 JUN 2015
Accepted 8 DEC 2015
Accepted article online 13 DEC 2015

Abstract Seasonally dry ecosystems exhibit periods of high water availability followed by extended intervals during which rainfall is negligible and streamflows decline. Eventually, such declining flows will fall below the minimum values required to support ecosystem functions or services. The time at which dry season flows drop below these minimum values (Q_*), relative to the start of the dry season, is termed the "persistence time" (T_{Q_*}). The persistence time determines how long seasonal streams can support various human or ecological functions during the dry season. In this study, we extended recent work in the stochastic hydrology of seasonally dry climates to develop an analytical model for the probability distribution function (PDF) of the persistence time. The proposed model accurately captures the mean of the persistence time distribution, but underestimates its variance. We demonstrate that this underestimation arises in part due to correlation between the parameters used to describe the dry season recession, but that this correlation can be removed by rescaling the flow variables. The mean persistence time predictions form one example of the broader class of streamflow statistics known as crossing properties, which could feasibly be combined with simple ecological models to form a basis for rapid risk assessment under different climate or management scenarios.

1. Introduction

Pronounced variability in precipitation is the defining characteristic of seasonally dry ecosystems (SDE) [*Fatichi et al*., 2012; *Vico et al*., 2014], which cover nearly 30% of the planet and contain about 30% of the Earth's population [*Peel and Finlayson*, 2007; *CIESIN*, 2012]. In these regions, a distinct rainy season is followed by a pronounced dry season during which rainfall makes a small or negligible contribution to the water balance. As a consequence, the availability of dry season surface water resources depends strongly on streamflow, which is generated primarily from the storage and subsequent discharge of antecedent wet season rainfall in the subsurface [*Brahmananda Rao et al*., 1993; *Samuel et al*., 2008; *Andermann et al*., 2012]. Because these transient stores are strongly influenced by the characteristics of the wet season climate, dry-season water availability can be highly variable from year to year in many SDE's [*Samuel et al*., 2008; *Andermann et al*., 2012]. This hydroclimatic variability leaves SDE's, considered important "hot spots" of biodiversity [*Miles et al*., 2006; *Klausmeyer and Shaw*, 2009], and the human populations that depend upon them susceptible to threats, such as soil erosion, deforestation, and water diversions [*Miles et al*., 2006; *Underwood et al*., 2009]. Future climate scenarios are projected to further intensify wet season rainfall variability in many SDEs [e.g., *Gao and Giorgi*, 2008; *García-Ruiz et al*., 2011; *Dominguez et al*., 2012], necessitating models which can predict the response of water resources to climatic change in order to measure the corresponding risk to local ecosystems and human populations [*Vico et al*., 2014; *Müller et al*., 2014].

Stochastic methods have a 30 year history of use in deriving simple, process-based models for the probability distributions of hydrologic variables, such as soil moisture, streamflow, and associated ecological responses [*Milly*, 1993; *Szilagyi et al*., 1998; *Rodriguez-Iturbe et al*., 1999; *Laio*, 2002; *Botter et al*., 2007; *Thompson et al*., 2013, 2014]. To date, the majority of stochastic analytical models for hydrology have been developed under conditions where the climatic forcing does not exhibit strong seasonality [*Rodriguez-Iturbe et al*., 1999; *Porporato et al*., 2004; *Botter et al*., 2007]. Those studies that have considered the effects of seasonality in rainfall or evaporative demand have either focused on the mean dynamics of the variable of interest [*Laio*, 2002; *Feng et al*., 2012, 2015] or excluded a treatment of the transient dynamics between the wet and dry seasons [*D'odorico et al*., 2000; *Miller et al*., 2007; *Kumagai et al*., 2009]. This is problematic in

situations when such transient hydrologic dynamics have a large impact on the availability of water—i.e., in SDEs [*Viola et al*., 2008; *Müller et al*., 2014; *Feng et al*., 2015]. Recently, stochastic analytical models for streamflow and soil moisture have been extended to include seasonal transitions in SDEs [*Viola et al*., 2008; *Feng et al*., 2012; *Müller et al*., 2014; *Feng et al*., 2015]. In the case of streamflow models, this is accomplished by explicitly accounting for the dynamics of the seasonal streamflow recession during the dry season [*Müller et al*., 2014].

In SDE's, the question, "how long do dry season streamflows persist above a given level?" is highly pertinent to the habitat quality and ecological functions sustained by streams, and to the legal and management frameworks applied to support those functions. For example, ecosystem managers often assume a correspondence between habitat availability and the stream wetted perimeter in order to determine critical minimum flow values (below which in-stream conditions become suboptimal for habitat protection), [e.g., *Nelson*, 1980; *Annear and Conder*, 1984; *Parker and Armstrong*, 2001]. These minimum flows are frequently adopted as regulatory measures, and thus set conditions beyond which in-stream water abstractions are prohibited. Other ecological transitions are also flow-dependent; for instance, lower bed-shear stresses associated with low flows are suspected to promote blooms of toxic cyanobacteria in some northern California watersheds [*Power et al*., 2015] (K. Bouma-Gregson, personal communication, 2015). The flow regime also appears to be the primary determinant for temperature-driven stratification of deep river pools, with implications for organisms that depend on these pools for summer survival [*Nielsen et al*., 1994; *Turner and Erskine*, 2005].

A number of statistical and deterministic modeling methods have been developed to characterize low flow conditions in both gauged and ungauged basins [*Nathan and McMahon*, 1992; *Skøien et al*., 2006; *Müller and Thompson*, 2015; *Ganora et al*., 2009; *Castellarin et al*., 2007; *Laaha and Blöschl*, 2007; *Arnold et al*., 1998, among others]. Regression-based and geostatistical techniques employ the concept of hydrologic similarity—the idea that catchments with similar geomorphologic and hydroclimatic features should also exhibit similar low flow features [*Blöschl et al*., 2013]. Deterministic rainfall-runoff models [e.g., *Arnold et al*., 1998] can be used for low flow estimation, though such models cannot provide a probabilistic characterization without computationally intensive Monte Carlo techniques.

Compared to their statistical and deterministic counterparts, process-oriented stochastic methods possess a number of advantages. Their simplicity facilitates applications even when data are sparse, and their mechanistic underpinnings overcome the limitations of statistical models which cannot, for example, distinguish between the effects of a nonstationary climate and shifts due to land use change. It is also notable that these stochastic models typically yield analytic PDF outputs with physically interpretable parameters. Such expressions conveniently lend themselves to applications in risk-oriented frameworks. For example, a related stochastic hydrologic model for soil moisture has been applied to assess plant pathogen risk at the regional scale [*Thompson et al*., 2013, 2014]. Analogous streamflow methods to estimate ecological risks based on climate and stream characteristics could provide a toolkit for assessing the condition of existing riverine ecosystems, as well as their vulnerability under alternative climatic, land use, or management scenarios.

This study aims to develop a model that would support such risk assessment by predicting the probabilistic character of the *persistence time*. The persistence time, denoted T_{Q_*}, is the length of the period that the dry season streamflow remains above a given flow threshold (Q_*). The distribution of T_{Q_*} links wet season climatic variation and land use (via vegetation water demand) to dry season recession characteristics.

Using the frameworks derived by *Botter et al*. [2007] and *Müller et al*. [2014] to characterize the wet season flow dynamics and the transition to the dry season, respectively, we derived analytical expressions for the probability distribution function (PDF) of T_{Q_*} and its expectation. The model is defined for rivers in seasonally dry climates; for this definition to be met, there must be a significant reduction in flow between mean wet season conditions and the dry season behavior. This condition may be violated in managed rivers (e.g., when dam releases elevate dry season flows) or in watersheds with significant groundwater contributions, which may be sufficient to smooth out flow variations even on seasonal scales. The model was validated using a multiyear streamflow data set from the United States Geological Survey's network of stream gages.

Applying stochastic methods to predict empirical discharge signatures, such as the persistence time, aligns with a recent review of prediction in ungauged basins, which explicitly notes the utility of probabilistic

streamflow models and calls for more research efforts to characterize their merits and limitations [*Blöschl et al*., 2013]. With this in mind, our model validation demonstrates two important results concerning stochastic methods, one "positive" and one "negative":

1. The positive result that the mean persistence time can be identified well as a function of wet season rainfall statistics and seasonality statistics; allowing the use of analytical models to predict the expected dry season flow persistence.
2. The negative result that the variance of the persistence time PDF is underestimated, highlighting the significance of variations in the parameters defining the recession.

We demonstrate that the underestimation of the persistence time variability arises due to fluctuations and correlation between the parameters of the power law model used here (and in many other studies, e.g., *Tague and Grant* [2004]; *Kirchner* [2009]; *Botter et al*. [2009]) to characterize the dry season recession. This correlation is not physical, but is an inevitable artifact arising from the properties of power laws. Using an existing power law parameter de-correlation technique [*Bergner and Zouhar*, 2000; *Mather and Johnson*, 2014], we quantified the effect of this correlation on our predictions, and demonstrated substantial improvement in the model predictions once it was removed. These simulations motivate further investigation into recession parameter variability; a more thorough understanding of the origins of this behavior is crucial for the continued development of minimal, process-oriented stochastic models.

2. Methods

2.1. Definition of Symbols and Terms

Throughout this section, $\Gamma(*)$ represents the gamma function and $\Gamma(*,*)$ represents the upper incomplete gamma function. The probability density function (PDF) is represented by p and the cumulative density function (CDF) by P. Subscripts, in upper case, denote the random variable being described by the PDF or CDF, and the corresponding lower case characters denote the observed value of the random variable. For example, the PDF and the CDF of stream discharge Q at value q are written $p_Q(q)$ and $P_Q(q)$, respectively.

2.2. Modeling Approach

The process by which we derive expressions for the mean persistence time and the persistence time probability distribution is illustrated in Figure 1. First, the year is partitioned into a wet and dry season, shown in Figure 1a. The steady state wet season flow PDF (Figure 1b) is obtained from the work of *Botter et al*. [2007], which is used to derive the probability distribution function describing the streamflow at the start of the dry season/end of the wet season (Figure 1c). This streamflow provides the initial condition for a deterministic recession during the dry season, allowing the probability distribution for the initial condition to be transformed into a probability distribution for the recession persistence time (Figure 1d). These steps are outlined in the next sections.

2.2.1. Steady State Wet Season Streamflow Distribution

The steady state, wet season streamflow PDF derived by *Botter et al*. [2007] forms the point of departure for this analysis. Assuming that recharge events can be described by a marked Poisson process with frequency (λ [1/T]) and mean depth ($1/\gamma_Q$, where γ_Q has units of [T/L^3]), and that the catchment residence time distribution is also exponential, with mean $1/k$ [T], the PDF for wet season streamflow (Q_w) follows a gamma distribution:

$$p_{Q_w}(q_w) = \frac{\gamma_Q^m}{\Gamma(m)} q_w^{m-1} \exp\left(-\gamma_Q q_w\right). \tag{1}$$

For an exponential catchment residence time distribution, the streamflow recession is appropriately modeled using a linear recession model, $dQ/dt = -kQ$, where k is the inverse of the mean residence time, also known as the streamflow recession constant. Here, the dimensionless parameter m [ ] is the ratio between the mean catchment residence time ($1/k$ [T]) and the mean interarrival time ($1/\lambda$ [T]) of the recharge events. The distribution of recharge depths (exponential with rate parameter γ_Q) can also be computed from catchment soil, vegetation, and hydroclimatic parameters, assumed to be homogeneous across the catchment [*Botter et al*., 2007; *Müller et al*., 2014].

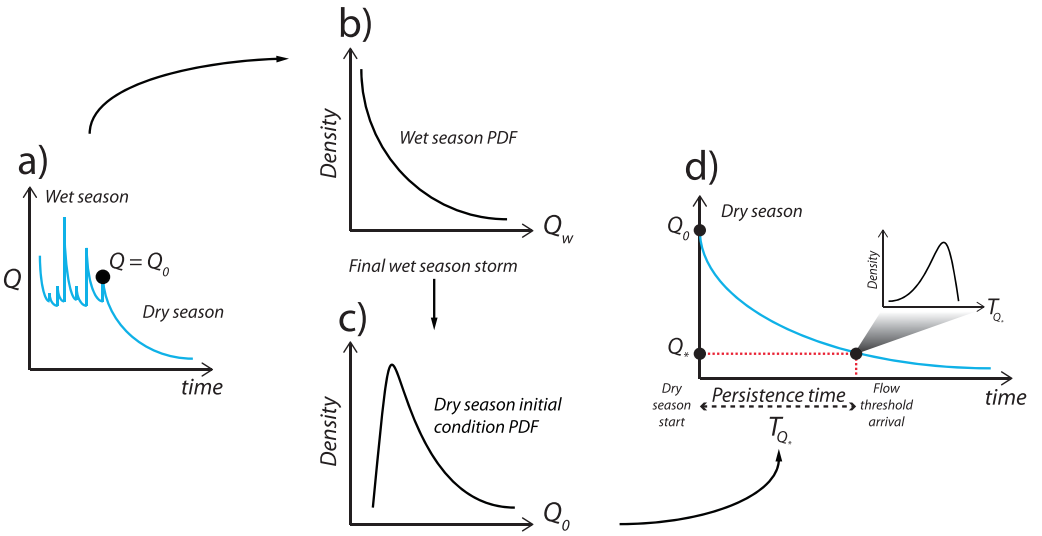

Figure 1. Conceptual illustration of the persistence times model. The year is partitioned into a wet and dry season (a). The wet season probability distribution (b) is determined according to the model of *Botter et al.* [2007]. The peak flow distribution from the wet season model is used to represent the probability distribution (c) of the dry season initial discharge condition (the discharge following the final storm of the wet season). Through the nonlinear recession relationship (equation (5)), the recession persistence time random variable is computed as a derived random variable of the (stochastic) dry season initial condition (d).

2.2.2. Streamflow Conditions at the End of the Wet Season

In order to uniquely determine the persistence time above a given flow threshold, the initial flow condition (Q_0) at the beginning of the dry season must be specified. Under the simplifying assumption that rainfall seasonality is perfectly binary [*Müller et al.*, 2014], we can mark the start of the dry season as the last recognizable streamflow peak of the wet season. In practice, the selection of this final peak is nontrivial due to the fact that seasonality is not perfectly binary. Section 2.3 develops a consistent methodology to determine the time at which this final wet season peak occurs. At the time of occurrence of this final peak, total discharge is the sum of two stochastic processes: (1) the discharge at the time of the arrival of the last wet season storm and (2) the flow increment generated by the last wet season storm, which we denote Δ. The memory-less property of the Poisson process implies that the discharge at the arrival of the final wet season storm is simply described by the PDF of wet season flow, p_{Q_w}. The initial condition random variable is therefore given by the sum:

$$Q_0 = Q_w + \Delta, \tag{2}$$

where the flow increment (Δ) is exponentially distributed with mean $1/\gamma_Q$ [*Botter et al.*, 2007]. Provided that the random variables are independent, the distribution for Q_0 is then the convolution of p_Δ and p_{Q_w}:

$$p_{Q_0}(q_0) = \int_0^{q_0} p_{Q_w}(q_w) \cdot p_\Delta(q_0 - q_w)\, dq_w = \frac{\gamma_Q^{m+1}}{\Gamma(m+1)} q_0^m \exp\left(-\gamma_Q q_0\right), \tag{3}$$

which is also gamma distributed with rate γ_Q and shape parameter $m + 1$.

2.2.3. The Seasonal Recession

Throughout the large draw-down in catchment storage that occurs during the dry season, the nonlinear nature of the recession dynamics cannot be ignored and the use of a linear reservoir model for the streamflow recession is not appropriate [*Brutsaert and Nieber*, 1977]. We instead describe the dry-season recession with the nonlinear relation:

$$\frac{dQ_d}{dt} = -aQ_d^{1-r}, \tag{4}$$

where Q_d is the dry season streamflow, a is the recession scale parameter, and r is a recession exponent parameter. For an initial streamflow condition, Q_0, this nonlinear, ordinary differential equation can be solved for Q_d:

$$Q_d(t) = (Q_0^r - art)^{\frac{1}{r}}. \tag{5}$$

This form typically well-approximates flow recessions and is supported by multiple theories, which predict that the first-order dynamics of the streamflow recession take a power law form [*Brutsaert and Nieber*, 1977; *Harman et al*., 2009; *Biswal and Marani*, 2010]. For most practical cases, the recession exponent (1–*r*) is greater than or equal to one ($r \leq 0$) and the units of the recession coefficient (*a*) depend on the value of the fitted exponent, which can be determined through empirical fitting procedures or chosen from theoretical considerations. These parameters are also known to vary seasonally, interannually, and across individual recession events [*Kirchner*, 2009; *Biswal and Marani*, 2010; *Botter et al*., 2013; *Bart and Hope*, 2014; *Basso et al*., 2015]. Section 2.5 examines the potential impact of this form of variability on persistence times calculations.

2.2.4. The Persistence Time PDF, $p_{T_{Q_*}}(t_{Q_*})$

Due to the fact that Q_0 can be expressed as a single variable function of t_{Q_*}:

$$Q_0(t_{Q_*}) = \left(Q_*^r + art_{Q_*}\right)^{\frac{1}{r}}, \tag{6}$$

the persistence time PDF ($p_{T_{Q_*}}(t_{Q_*})$) can be obtained as a derived distribution of the dry season initial condition distribution ($p_{Q_0}(Q_0)$). Figure 1 illustrates the relationship between Q_0 and the persistence time via the recession relationship. By the properties of derived distributions, we find $p_{T_{Q_*}}(t_{Q_*})$ as:

$$p_{T_{Q_*}}(t_{Q_*}) = p_{Q_0}(Q_0(t_{Q_*}))\frac{dQ_0}{dt}\bigg|_{t_{Q_*}} = \frac{a\gamma_Q^{m+1}}{\Gamma(m+1)}\exp\left[-\gamma_Q\left(Q_*^r + art_{Q_*}\right)^{\frac{1}{r}}\right]\left(art_{Q_*} + Q_*^r\right)^{\frac{m-r+1}{r}}, \tag{7}$$

where $0 < t_{Q_*} < -Q_*^r/(ar)$. This positive upper bound on the domain of $p_{T_{Q_*}}$ stems from the fact that $Q_0 \to \infty$ as $t_{Q_*} \to -Q_*^r/(ar) > 0$. In other words, the streamflow recession relationship will always reach the chosen flow threshold in finite time, even in the limit of an infinitely high initial condition. Since the initial condition could be less than the chosen flow threshold ($Q_0 < Q_*$), the persistence time distribution is *also* defined for all negative real numbers. Nevertheless, as long as the chosen flow threshold value is not unreasonably large (less than 50% of the mean annual flow, for example), the proportion of the mass of the persistence time PDF associated with negative values for T_{Q_*} is negligible. To be precise, the truncation of $p_{T_{Q_*}}$ removes all probability mass for $T_{Q_*} < 0$, which is equal to the probability that the dry season initial condition is less than the chosen flow threshold, $Pr[T_{Q_*} < 0] = Pr[Q_0 < Q_*] = P_{Q_0}(Q_*)$. In all subsequent analyses, we truncate $p_{T_{Q_*}}$ for $T_{Q_*} < 0$, renormalize the persistence time distribution as $\frac{1}{1-P_{Q_0}(Q_*)}p_{T_{Q_*}}$ for $T_{Q_*} > 0$, and do not consider persistence time data for years when $Q_0 < Q_*$. In Appendix A, we demonstrate that even for relatively high flow thresholds, this condition occurs fewer than 10% of cases.

2.2.5. The Mean Persistence Time, $\mathbb{E}[T_{Q_*}]$

The direct integration of equation (7) to obtain an expression for the mean persistence time presents analytical difficulties. However, assuming that the peak flow at the end of the wet season exceeds the dry season flow threshold (Q_*), equation (6) can be inverted to obtain an expression for t_{Q_*} in terms of Q_0 and Q_*:

$$Q_* = (Q_0^r - art_{Q_*})^{\frac{1}{r}} \quad \Rightarrow \quad t_{Q_*} = \frac{Q_0^r - Q_*^r}{ar}. \tag{8}$$

The expression for t_{Q_*} is a function of the random variable, Q_0. We can then derive all the moments of this function using the distribution p_{Q_0}. For instance, the mean is given by:

$$\begin{aligned}\mathbb{E}[T_{Q_*}] &= \int_{Q_*}^{\infty} t_{Q_*} \cdot p_{Q_0}(Q_0)\, dQ_0 \\ &= \int_{Q_*}^{\infty} \frac{Q_0^r - Q_*^r}{ar} \cdot \frac{\gamma_Q^{m+1}}{\Gamma(m+1)} Q_0^m \exp\left(-\gamma_Q Q_0\right) dQ_0 \\ &= \frac{\Gamma(r+m+1, \gamma_Q Q_*) - (\gamma_Q Q_*)^r \Gamma(m+1, \gamma_Q Q_*)}{ar\gamma_Q^r \Gamma(m+1)}.\end{aligned} \tag{9}$$

While higher order moments, such as the variance, can be obtained, the expressions are unwieldy and are not presented here.

Table 1. Study Catchment Information

Catchment	USGS Gage ID	Stream	Drainage Area (km^2)	Years of Data (n_i)
C1	11463170	Big Sulphur Creek, Cloverdale, CA	33.9	31
C2	11143000	Big Sur River, Big Sur, CA	120.4	60
C3	11476600	Bull Creek, Weott, CA	72.8	49
C4	14325000	Coquille River, Powers, OR	437.7	81
C5	11475000	Eel River, Fort Seward, CA	5457.1	55
C6	11475560	Elder Creek, Branscomb, CA	16.8	43
C7	11481200	Little River, Trinidad, CA	104.9	49
C8	11481000	Mad River, Arcata, CA	1256.1	59
C9	11473900	Middle Fork Eel River, Dos Rios, CA	1929.5	45
C10	11468000	Navarro River, Navarro, CA	784.8	50
C11	11451100	North Fork Cache Creek, Clearlake Oaks, CA	155.9	39
C12	11468500	Noyo River, Fort Bragg, CA	274.5	59
C13	11472200	Outlet Creek, Longvale, CA	416.0	35
C14	11482500	Redwood Creek, Orick, CA	717.4	57
C15	11476500	South Fork Eel River, Miranda, CA	1390.8	71
C16	14307620	Siuslaw River, Mapleton, CA	1522.9	35

2.3. Model Parameter Estimation

We tested the persistence time derivations using U.S. Geological Survey daily discharge data for sixteen catchments in Northern California and Southern Oregon, as detailed in Table 1. These catchments are characterized by seasonally dry Mediterranean climates, in which the wet season and the "growing season" (i.e., summer, with highest insolation and temperature) are out of phase. These catchments exhibit a clear and dramatic separation between flow regimes, and strong seasonal recessions, making them a suitable set of catchments on which to test the model. Figure 2 shows the location of the test catchments, along with site photos and representative climate data.

Although it is possible to estimate λ and γ_Q from catchment vegetation, soil, and rainfall data, and to interpolate estimates of the linear recession constant k from neighboring gauges [*Müller and Thompson*, 2015], we did not test the persistence time model in ungauged basins. The difference in the quality of parameter estimates for the streamflow model when forced by stream data versus reliable rainfall data were explored in a previous study, and shown to be minimal [*Müller et al.*, 2014]. We therefore use gauged streamflow data to parameterize and to test the model.

To determine the parameters λ and γ_Q, we first identify all well-defined peaks from the wet season hydrograph (as defined below). λ is computed as the reciprocal of the mean of the interarrival periods between these peaks. Next, we extract the magnitude of the increasing segment of the hydrograph preceding each peak and compute γ_Q as the reciprocal of the mean of these positive discharge increments.

The remaining parameters to be estimated are the recession parameters, k for the wet season, and a and r for the dry season. To estimate these parameters, we first partitioned the year into distinct wet and dry periods. This was achieved by fitting a square wave function to each year of streamflow data, taking a value of the mean seasonal streamflow in each case. This fit was constrained by the requirement that the initial guess for the "wet season" should include both the centroid (along the time axis) of the annual streamflow time series:

$$\tau_Q = \frac{\int_0^{365} t \cdot Q(t)dt}{\int_0^{365} Q(t)dt}, \tag{10}$$

and the deviation about the centroid, $\tau_Q \pm s_Q$, where s_Q is defined as the square root of the second moment of the annual streamflow time series:

$$s_Q = \sqrt{\frac{\int_0^{365} (t-\tau_Q)^2 \cdot Q(t)dt}{\int_0^{365} Q(t)dt}}. \tag{11}$$

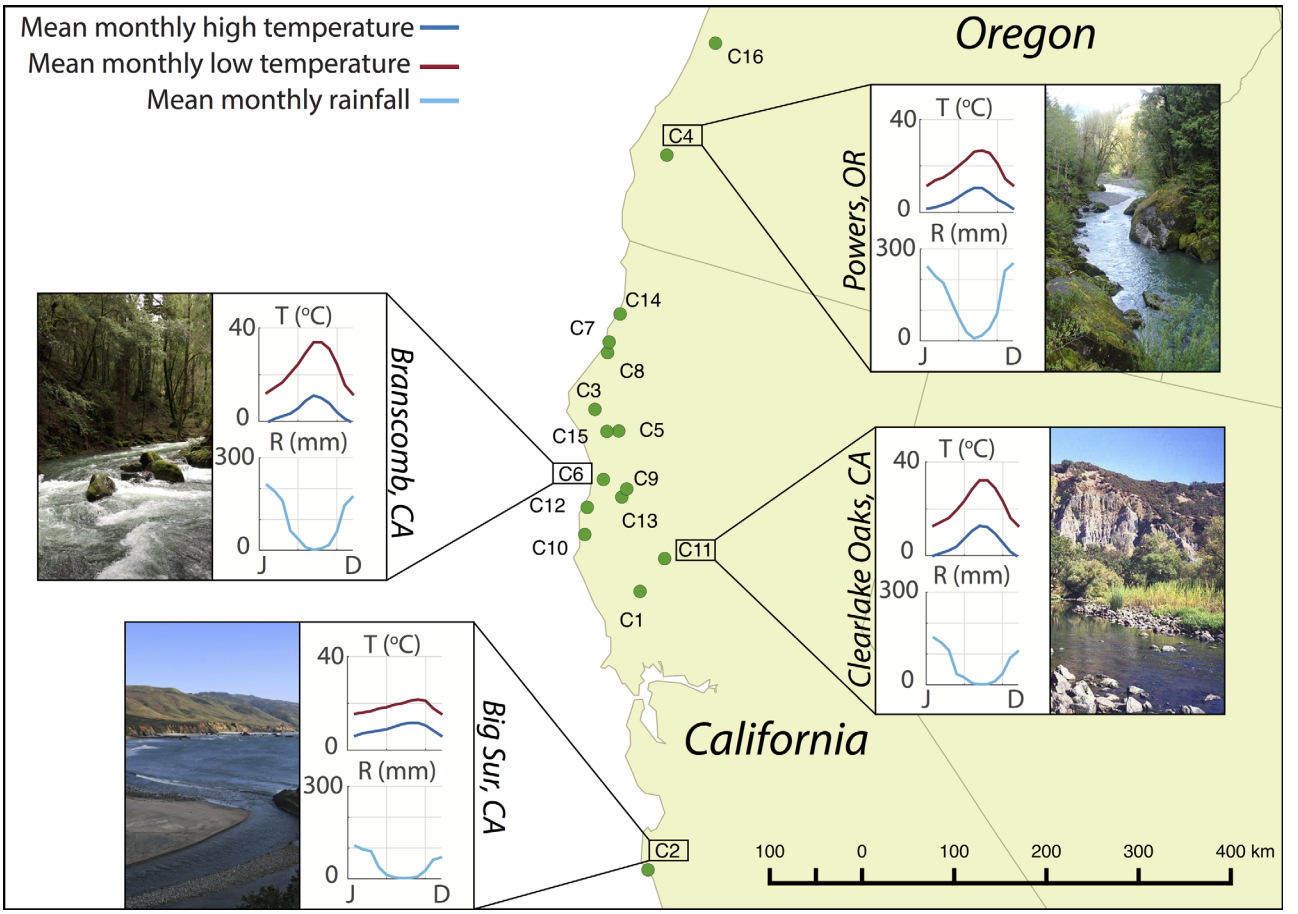

Figure 2. Map with study catchments. Insets with monthly averages of high temperature, low temperature, and precipitation totals for the Big Sur River (Big Sur, CA), Elder Creek (Branscomb, CA), the North Fork Cache River (Clearlake Oaks, CA), and the Coquille River (Powers, OR).

To estimate the dry season parameters, we first isolated the seasonal recession by identifying the last storm that initiated the seasonal dry down. In most cases, this storm was linked to the final streamflow peak in the fitted "wet season" square wave. In some cases, however, late spring storms resulted in larger streamflow peaks occurring in the initially fitted "dry season" period. The seasonal recession in these cases was taken to begin with the last of these peaks. The dry season duration (T_d) was then defined as the period between the start of the seasonal recession, and the rising edge of the fitted step function for the following year. Generally, T_d exceeded 150 days in all the study catchments. We used the first $T_d - 30$ days of the dry season to fit the recession parameters, a and r. The final 30 days were excluded because (i) gauged estimates of extreme low flows typically observed late in the dry season are often unreliable or recorded as zero, and (ii) we wished to exclude the seasonal transition from dry to wet in the fitting procedure to avoid early season storms in the following wet season. An alternative method to avoid end of dry season issues would be to fit a and r only to the recession periods greater than the threshold, Q_*. In this case, however, the fitted values a and r may then depend, albeit weakly, on the particular choice of threshold. This alternative method would undoubtedly generate better model performance, as only the relevant portion of the recession time series would be used for fitting. Nevertheless, this study implements the first method to ensure fitted values of a and r remain constant, regardless of the choice of threshold.

The wet season recession constant, k, was estimated by extracting all wet season flow recessions exceeding 4 days in length, and regressing the logarithm of the recession discharge against time. k was computed as the median of the regression slope coefficients across all extracted recessions.

The recession parameters (a and r) were fitted using a nonlinear least squares procedure, minimizing the sum of squared errors between the dry season recession model and the observed dry season recession over all years. Supporting information includes a table of these parameters for each catchment.

2.4. Model Evaluation

Having estimated the model parameters, persistence times were estimated for each year by considering a range of flow thresholds, finding the date at which those thresholds were first crossed during the seasonal recessions, and computing the time lapsed since the last wet season storm. Persistence times cannot be computed in this way for two cases:

1. For years when the flow threshold (Q_*) exceeded the dry season initial condition (Q_0). We do not expect this restriction to affect the quality of the streamflow data set; even for the highest flow threshold at 50% of mean annual flow, this condition accounted for less than 5% of the study years (see Appendix A for more details).
2. For years when the dry season discharge does not drop below the chosen flow threshold. Unless a river explicitly runs dry during the dry season, it will always be possible to define flows so low that the seasonal recession does not achieve these levels in a meaningful timeframe, that is, within the duration of a typical dry season.

To ensure that the model is only evaluated for meaningful flow thresholds (namely, flows that are low enough to be distinct from the wet season, but high enough that the river flow will pass below them in a typical dry season), we evaluate the model for thresholds (Q_*) ranging from 5% to 50% of mean annual flow.

The analytic mean persistence times were plotted against empirical mean persistence times for flow thresholds ranging from 5% to 50% of mean annual flow, and the corresponding R^2 value of a one-to-one line reported. The performance of the model in estimating persistence time PDFs was evaluated using the Nash-Sutcliffe Coefficient (NSC) as applied to the persistence time percentiles:

$$\mathrm{NSC} = 1 - \frac{\sum_{i=1}^{99} \left(\hat{T}_i - T_i\right)^2}{\sum_{j=1}^{99} \left(T_j - \frac{1}{99}\sum_{k=1}^{99} T_k\right)^2}, \tag{12}$$

where $\hat{T}_i$ and T_i are the empirical and modeled persistence times associated with percentile i, respectively. The NSC corresponds to an R^2 value for the fit of a one-to-one line to a plot of the empirical percentiles versus the modeled percentiles; it has been used extensively for the assessment of hydrologic models [*Nash and Sutcliffe*, 1970; *Castellarin et al*., 2004; *Müller et al*., 2014]. NSC values range from negative infinity to one, where an NSC of one corresponds to a perfect match between the percentiles. Due to the strong dependence of the persistence times model on the performance of the wet season model, we also computed NSC values testing the wet season streamflow distribution (p_{Q_w}) and the dry season initial condition distribution (p_{Q_0}). Although this application of NSC values was originally developed for flow duration curves, the tests here are directly analogous to the duration curve, being derived from the PDFs. We thus assume NSC values provide a suitable relative rating scheme.

Supporting information provides illustrations of the analytic mean persistence times plotted against empirical mean persistence times, and plots of the persistence time PDFs for all catchments with Q_* set to 20% of mean annual flow.

2.5. Effect of Recession Variability on Predictions

As shown in section 3, the mean persistence time predictions perform well for most watersheds, yet the distributions $p_{T_{Q_*}}$ fail to reproduce the variance of the full empirical persistence time distributions. To determine why this occurred, we systematically assessed whether the model assumptions were met by the empirical data. In agreement with other recession studies, we found that the nonlinear recession parameters a and r varied significantly between years [*Kirchner*, 2009; *Biswal and Marani*, 2010; *Shaw and Riha*, 2012; *Botter et al*., 2013; *Bart and Hope*, 2014; *Basso et al*., 2015]. In violation of the model assumptions, which presume parameter independence, this variation was characterized by a strong correlation between a and r, which has not been examined in previous recession studies. An example of this correlation is shown for one of the study sites, Redwood Creek, in Figure 3 (left hand plot).

Such correlation has been identified in other studies as a mathematical artifact that arises from the scale-free properties of the power law (i.e., equation (4)), and existing techniques are available to rescale the flow variable Q to remove this correlation [*Bergner and Zouhar*, 2000]. The genesis of this artifact, and the theory

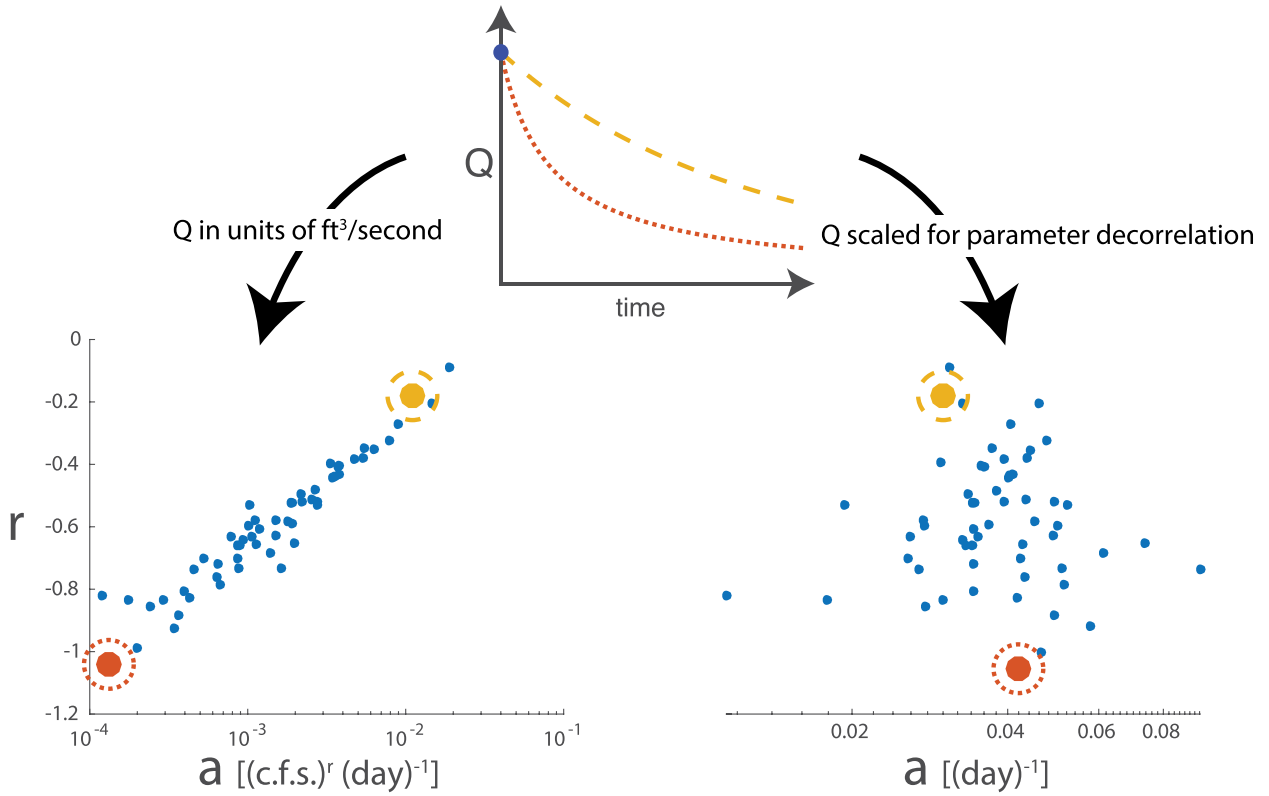

Figure 3. Fitted recession parameters for streamflow in units of cfs and dimensionless *Q* scaled to remove parameter correlation. The two highlighted parameter pairs correspond to the two recession curves illustrated in the smaller inset plot.

underpinning its removal, are outlined in Appendix B. The effectiveness of the rescaling technique in removing the correlation is illustrated in Figure 3 (right hand plot). Two recession curves, which correspond to the two highlighted recession parameter pairs, are plotted in the top of Figure 3. Section 4.1 provides more background and motivation for the examination of power law parameter correlation. First, however, we outline a method to quantitatively demonstrate the effects of recession parameter variability.

2.5.1. Monte Carlo Simulation

The persistence time derivations could be generalized to include recession parameter variability. This would require the specification of a joint PDF for the recession parameters ($p_{A,R}(a,r)$) and the integration of equation (7), the persistence time distribution, over this joint PDF. While this approach is elegant, the specification of $p_{A,R}(a,r)$ is a serious challenge. Using a – r data to generate an empirical, joint distribution is difficult, considering our small sample sizes (on the order of tens of years of dry season recession data per catchment). From a modeling standpoint, the determination of $p_{A,R}(a,r)$ from first principles would require a clear understanding of the mechanisms underlying recession parameter variability, a question which remains largely unanswered [*Harman et al.*, 2009], especially when variations in both a and r are considered.

In light of these challenges, we apply a Monte Carlo approach to assess the effects of recession parameter variability and correlation, both separately and in combination, on the predictions of the persistence time PDF.

To isolate the effects of the recession parameters and their variation, we first fit unique recession curves to each of the n_j observed dry season recessions for catchment j. This process generates n_j unique recession parameters pairs for each catchment, $\{(a_1,r_1),(a_2,r_2),\ldots,(a_{n_j},r_{n_j})\}$. We also compute a set of minimally correlated recession parameter pairs, denoted $\hat{a}, r$, by repeating the fitting procedure to flow data that had been rescaled using the parameter decorrelation method described in Appendix B [*Bergner and Zouhar*, 2000; *Mather and Johnson*, 2014]. Then, we fit a gamma distribution to the empirical initial conditions Q_0 on each recession. For a given Monte Carlo run, we draw n_j samples from this distribution. We use the fitted

rather than the modeled p_{Q_0} PDF in order to confine any model error sources to the treatment of a and r variation. The Monte Carlo proceeds by drawing a sample of Q_0, and computing a persistence time (using Q_* set to 20% mean annual flow). Four different treatments of a and r allow us to assess the effects of a and r variability and correlation on persistence time predictions:

1. **M1: constant *a* and *r*** The original scaling of Q (units of ft^3/s) was used. Persistence times were computed for each sampled n_j initial condition using constant values of a and r. The values of a and r for each catchment were chosen by minimizing the sum of squared errors between observed and the predicted dry season recessions over all years as described in section 2.3. This is a null case that replicates the developments in this paper. It contains neither variability nor correlation in the recession parameters.
2. **M2: varying but independent *a* and *r*** Again, the original scaling of Q in units of ft^3/sec is used. In contrast to M1, the recession parameters are now allowed to vary between each initial condition selected. The recession parameters are selected by bootstrapping independent samples from the sets $\{a_1, a_2, \ldots, a_{n_j}\}$ and $\{r_1, r_2, \ldots, r_{n_j}\}$. This case preserves variability but does not incorporate the observed correlation in the recession parameters. Additionally, the results from this simulation provide a reference which can be used to determine the relative benefit of implementing recession parameter decorrelation (M3).
3. **M3: Parameter decorrelation with varying, but independent, $\hat{a}$ and $\hat{r}$.** In this instance, Q is rescaled according to the decorrelation technique of *Bergner and Zouhar* [2000]. Persistence times are computed from the n_j initial conditions using new recession pairs generated by bootstrapping independent samples from the sets $\{\hat{a}_1, \hat{a}_2, \ldots, \hat{a}_{n_j}\}$ and $\{r_1, r_2, \ldots, r_{n_j}\}$. This case preserves variability, and accounts for the component of correlation in the recession parameters that can be removed by the *Bergner and Zouhar* [2000] method. It is notable that the *only* difference between M2 and M3 is the scaling of Q. Differences between the results of M2 and M3 explicitly illustrate the impact of recession parameter correlation.
4. **M4: Parameter decorrelation with varying, jointly sampled $\hat{a}$ and *r* pairs.** Q is nondimensionlized according to the decorrelation technique of *Bergner and Zouhar* [2000]. Persistence times are computed from the n_j initial conditions using recession pairs uniformly sampled (without replacement) from $\{(\hat{a}_1, r_1), (\hat{a}_2, r_2), \ldots, (\hat{a}_{n_j}, r_{n_j})\}$. This case preserves variability and all correlation in the recession parameters. If the decorrelation procedure completely removed all correlation of the form generated by the scale-dependent artifact (outlined in Appendix B), then there would be no measurable differences between M3 and M4, unless there exists another (physically derived) form of correlation between the recession parameter pairs; that is, correlation that does not obey the form of the artifactual correlation.

For each run of the process, a distribution of persistence times was generated, and compared to the empirical distribution via the NSC. The Monte Carlo process was repeated 1000 times to generate confidence intervals around the computed NSC's.

Table 2. Study Catchment Evaluation Metrics for the Wet Season Flow PDF (p_{Q_w}), the Dry Season Initial Condition PDF (p_{Q_0}), and for the Modeled Mean Persistence Times ($\mathbb{E}[T_{Q_*}]$)

Catchment	NSC for p_{Q_w}	NSC for p_{Q_0}	R^2 for $\mathbb{E}[T_{Q_*}]$
C1	0.8	0.94	0.93
C2	0.93	0.78	0.41
C3	0.89	0.88	0.96
C4	0.97	0.71	0.98
C5	0.94	0.76	0.88
C6	0.88	0.88	0.9
C7	0.96	0.58	0.98
C8	0.93	0.79	0.95
C9	0.81	0.76	0.9
C10	0.9	0.9	0.99
C11	0.78	0.92	0.85
C12	0.9	0.7	0.97
C13	0.87	0.8	0.77
C14	0.97	0.71	0.96
C15	0.91	0.81	0.98
C16	0.96	0.81	0.93

3. Results

3.1. Stochastic Streamflow Model Applied to Northern California and Southern Oregon Catchments

The wet season and dry season initial condition models performed well for the study catchments, as shown in Table 2. For the wet season model, all Nash Sutcliffe coefficients exceeded 0.75. With four exceptions (catchments C4, C7, C12, and C14, where $0.5 < \text{NSC} < 0.75$), the same holds true for the dry season initial condition. The initial condition models in these four catchments overpredicted the magnitude of the dry season initial condition.

3.2. Mean Persistence Time and its PDF

The ability of the persistence time model to predict the mean persistence time was good

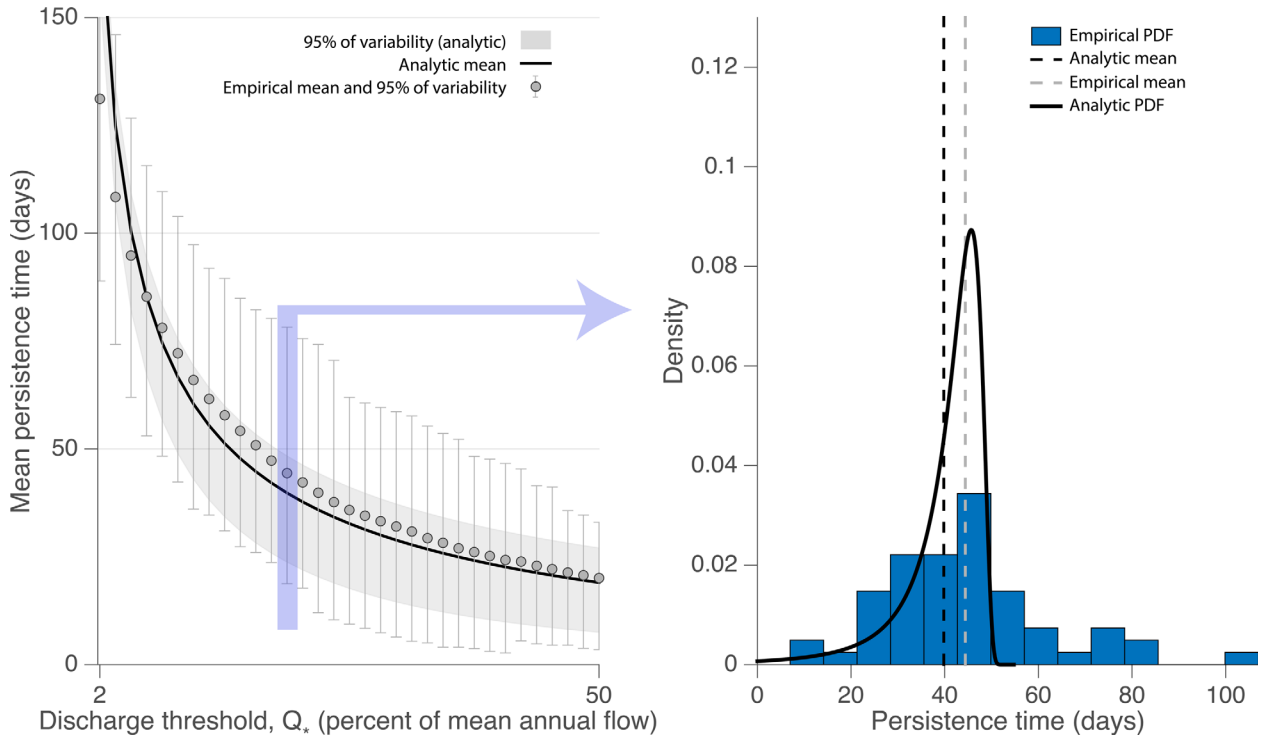

Figure 4. The empirical mean persistence time plotted against the analytic mean persistence time for Redwood Creek (a). The gray envelope signifies 95% of the variability around the analytic mean persistence times, whereas the gray whiskers represent 95% of the variability around the mean empirical persistence times. (b) The full persistence time distribution for a discharge threshold set to 20% of mean annual flow. Blue boxes represent the empirical histogram and the solid black line plots the analytic probability distribution. The empirical (gray-dashed) and analytic (black-dashed) means are also shown in Figure 4b.

(NSC $>$ 0.75) for discharge thresholds ranging from 5% to 50% of mean annual flow (Table 2). One exception is for catchment C2 (Big Sur), where the model performance is relatively poor.

In Figure 4a, a comparison of the predicted and observed mean persistence times for the threshold range 2%–50% of mean annual flow is shown for catchment C14, Redwood Creek. The fit here is typical for most catchments, where the mean performance is excellent for larger flow thresholds, and begins to degrade once the flow threshold approaches 2% mean annual flow (larger persistence times). Generally, mean performance across all catchments tends to break down at very low discharge thresholds. As noted in 2.4, this is because seasonal recessions cannot achieve very low flow thresholds within the dry season duration; that is, the following wet season begins before the threshold is reached. In this case, persistence times can only be computed for the driest years, and so are biased towards smaller values. Catchment C2 (Big Sur) performs especially poorly (a breakdown of the model for flow thresholds near 20% of mean annual flow), likely due to the fact that Big Sur has significant geothermal flows generated by three distinct springs. In this watershed, dry season flows rarely drop below 20% mean annual flow.

Figure 4a highlights the variability around the mean for both the analytic (gray envelope) and empirical (gray whiskers) mean persistence times. The spread of the analytic curve demonstrates a clear skew toward shorter persistence times, whereas the empirical curve shows a fairly symmetric spread about the mean. Persistence time distributions at 20% of the mean annual flow (blue rectangle in Figure 4a) are plotted in Figure 4b (PDFs at this threshold are presented for all other catchments in supporting information). At this threshold, it is clear that the analytic persistence time distribution underestimates the observed variability. Based on the model derived here, moreover, the analytic persistence time distribution is undefined for persistence times outside the interval, $0 < t_{Q_*} < -Q_*^r/(ar)$. The empirical distribution does not adhere to this domain restriction. Some of the observed persistence times are more than twice as large as the maximum possible persistence time predicted by the analytic distribution. Across all flow thresholds and catchments explored here, the modeled persistence time variability underestimates the observed variability.

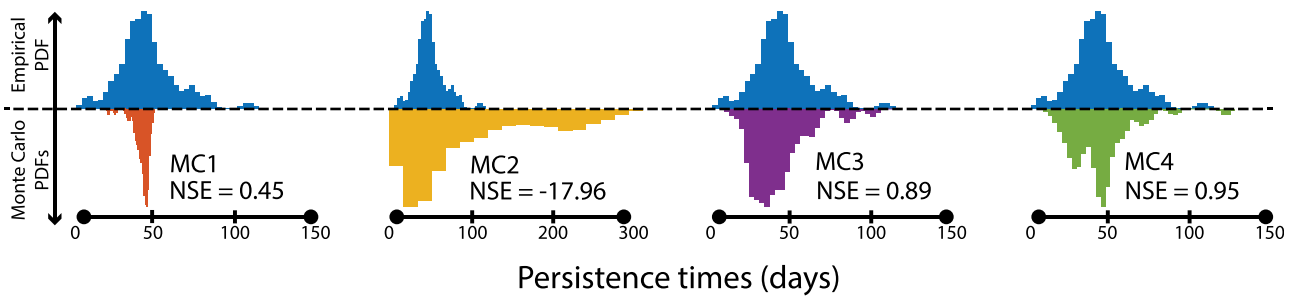

Figure 5. Results from a single Monte Carlo run for Redwood Creek. (top row) The blue PDF's represent the empirical persistence times data, while (bottom row) the multicolored PDF's on the each represent one of the four types of Monte Carlo simulation (M1–M4). The *y* axis scale is omitted to facilitate comparisons. Also note the scale for MC2, stretched due to the fact that this Monte Carlo simulation produces very large persistence times. NSC values for goodness of fit relative to the empirical persistence times are included for each simulated probability distribution.

3.3. Source of Persistence Time Variability

Example persistence time probability distributions generated from a single Monte Carlo run for Redwood Creek are presented in Figure 5. The results for simulation M1 echo those from the analytic distribution in Figure 4b. As expected, the mean performance is good, but the full variability (Figure 5, empirical data) is not well accounted for. Simulation M2 represents the case where parameters vary but the correlation between pairs is not preserved. In this case, almost all predictive ability is lost. Simulation M3 also relies on independent bootstrapping of parameters, but the streamflow is scaled (according to the technique of *Bergner and Zouhar* [2000]) to minimize any recession parameter correlation (specifically, parameter correlation that adopts a logarithmic dependence between parameters is eliminated; parameter correlation with a different functional dependence may remain). Here the model performance is quite reasonable, and greatly improved compared to both M1 and M2. Model M3 does not appear to perform as well as model M4 (which includes any correlation remaining after streamflow rescaling), though the difference in performance is not large.

These results are general for all the watersheds in the study, as shown in Figure 6. The primary conclusion is that the greater than expected spread in persistence time distributions results from the coupled interannual variability in the seasonal recession parameters, a and r. Without accounting for variability in the streamflow recession parameters (Figure 6, M1), the performances of the analytic PDFs are generally poor, with tight confidence intervals around the computed NSCs. Simulation M2 demonstrates that neglecting the recession parameter correlation within a power law model fundamentally violates the mechanics of the power law (such correlation is an inevitable and essential feature of power law functional models, see Appendix B) and leads to basically nonsensical results: poor model performance and wide confidence intervals on the computed NSCs. Merely rescaling the flow variables to remove the parameter correlation (M3) greatly improves model performance, although preserving the original recession parameter pairs (M4) continues to improve the model behavior. Disparities between M3 and M4 indicate that some form of residual parameter correlation remains, following the de-correlation procedure. As expected, simulation M4 performs very well, illustrating that recession parameter pairs are functionally independent of streamflow initial conditions—at least in terms of the impact on the persistence time PDFs.

4. Discussion

4.1. Model Performance

The proposed model for the persistence time during the summer dry season provides a robust estimate of the mean conditions at which flow in a drying river is sustained above meaningful threshold values. The model thus provides a reasonable basis for estimating the effects of changing climate or land use parameters on the mean availability of dry-season surface water resources, and the associated ecosystem services they provide. The minimal parameterization of the model would in principle facilitate distributed assessments across many small watersheds.

A full accounting of the variability in dry season streamflow properties clearly requires elucidating the PDF of persistence times, and the analytical model fails to achieve this. Mediocre fits in the dry season initial

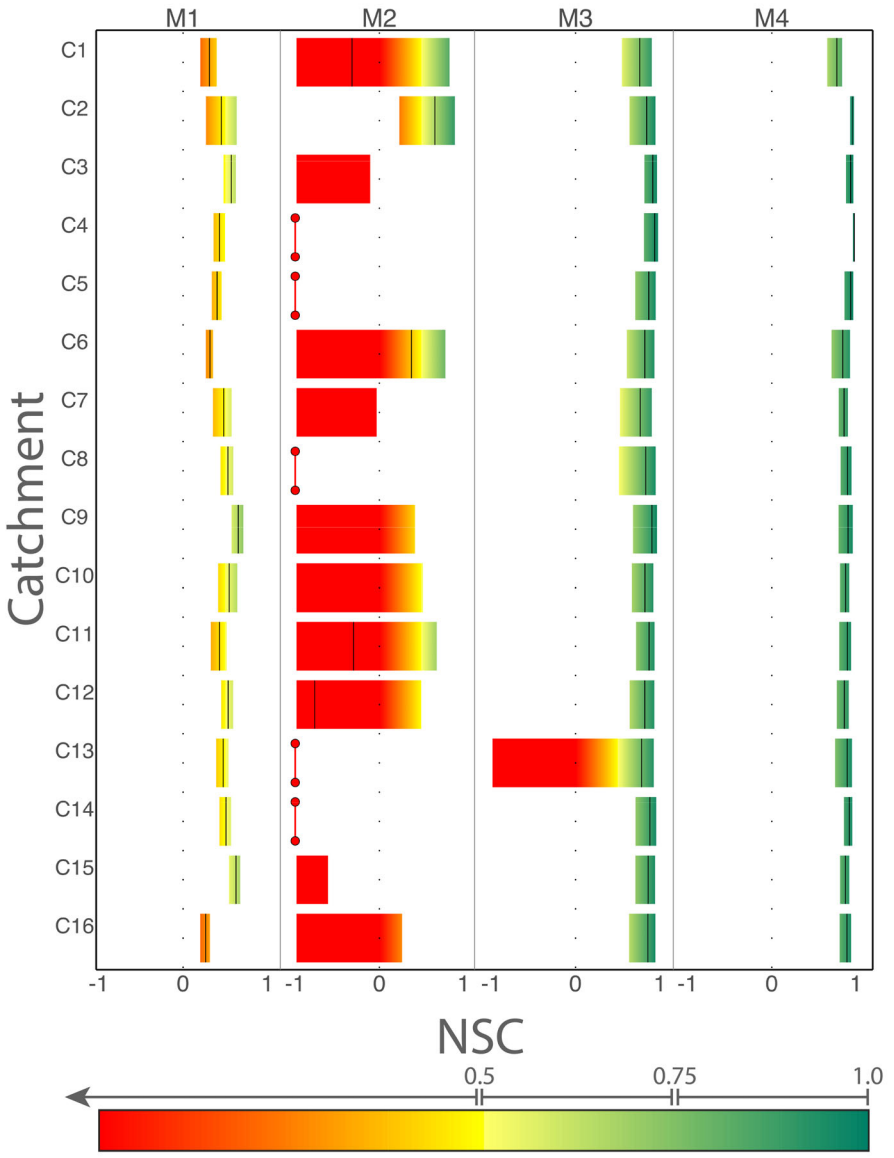

Figure 6. Results from the recession parameter Monte Carlo simulations. Each row corresponds to a study catchment, and each column corresponds to one of the four simulations. Mean Nash-Sutcliffe coefficients are represented with a vertical black line with a color bar corresponding to the 95% confidence interval of calculated NSC's; no black line indicates that the mean is less than −1. A red vertical line segment with black circles indicates that the calculated mean NSC and confidence intervals are less than −1. The colorbar scale indicates the relative quality of the fits according to the NSC value.

condition distribution cannot explain increased variability in the persistence times, unless the distributions of Q_0 themselves exhibited unexpected increases in variability, which they do not. The primary source of error in the initial condition distributions appears to be a slight bias towards smaller values of Q_0. This could be due to nonbinary seasonality (bias toward smaller storms toward the end of the wet season), or performance decreases associated with peak flow estimation using the linear recession model in the wet season [*Basso et al.*, 2015]. Monte Carlo simulations illustrate that it is interannual variation in the character of the seasonal recession that results in a large increase in the variability of persistence times, which is not well estimated with median recession characteristics. Unfortunately, such variation is generally not possible to prescribe a priori.

Physically, variation in recession behavior is thought to arise due to both changes in total catchment storage and in the partitioning of that storage amongst reservoirs with different drainage characteristics

[*Bart and Hope*, 2014; *Harman et al*., 2009; *Biswal and Marani*, 2010; *Shaw and Riha*, 2012; *Moore*, 1997]. To account for such variability in a lumped model requires specifying multiple reservoirs, each characterized by distinct timescales—a challenging basis from which to generate stochastic predictions. Fundamentally, the hydrologic literature lacks a unified understanding of the genesis of recession variability, which has been linked by various authors to the drainage dynamics of hillslope aquifers [*Brutsaert and Nieber*, 1977], to catchment heterogeneity [*Harman et al*., 2009], and to variability in the wetted extent of the channel network [*Biswal and Marani*, 2010]. Evidently, a single nonlinear reservoir model is inadequate to capture these variations and thus to represent the full probabilistic character of seasonal recessions.

Moreover, the parameter correlation identified in this analysis suggests that testing the existing theories regarding recession variability requires carefully controlling for the mathematical artifacts that the widely used power law recession models can generate. Many of the theories addressing recession characteristics attribute physical meaning to parameters in a power law recession model [*Harman et al*., 2009; *Biswal and Marani*, 2010, 2014; *Brutsaert and Nieber*, 1977]—and yet the values of these parameters, and their relationship to each other, appear to be poorly constrained.

As far as we are aware, the mathematical artifact leading to the $a - r$ correlation we observed is systematically removed in only a single study in the hydrological literature: using the technique from *Bergner and Zouhar* [2000], *Mather and Johnson* [2014] removed power law parameter correlation in order to improve the performance of a turbidity rating curve. In that work and here, recession parameter correlation presented an unexpected and significant source of model error. In other fields of study, ranging from fluid mechanics to materials science, power law parameter correlation has been mistakenly identified as having physical meaning [*Zilberstein*, 1992; *Cortie*, 1991; *Shih et al*., 1990; *Hussain et al*., 1999]. Power law parameter correlation has been observed but not properly identified or removed in few streamflow recession studies [*Krueger et al*., 2010; *McMillan et al*., 2014; *Sawaske and Freyberg*, 2014]. This is due, in part, to the fact that the classical goal of a recession analysis avoids event-specific recession analyses of $a - r$ point clouds. Nevertheless, parameter correlation should be accounted for, where appropriate, especially in light of rapidly increasing interest in recession parameter variability [*Shaw and Riha*, 2012; *Bart and Hope*, 2014; *McMillan et al*., 2014; *Biswal and Marani*, 2014; *Basso et al*., 2015; *Patnaik et al*., 2015].

4.2. Ecological Applications of Streamflow Crossing Statistics

The recession persistence time is one of a more general set of streamflow statistics known as the "crossing properties." The crossing properties of hydrologic variables, including soil moisture and streamflow, are known to be ecologically important [*Laio et al*., 2001; *Porporato et al*., 2001; *Botter et al*., 2008; *Doulatyari et al*., 2014; *Tamea et al*., 2011], but their scope of application has been primarily limited to the response of vegetation to disturbance (e.g., drought, flood, etc).

The persistence of flow above minimum thresholds during the dry season influences many ecological outcomes. For example, low-flow conditions can induce fragmentation of the channel network, impacting the mobility of resident stream fishes [*Thompson*, 1972; *Fullerton et al*., 2010; *Holmes et al*., 2015; *Hwan and Carlson*, 2015]. As mentioned in the introduction, the seasonal recession in some Northern California watersheds leads to a fall in the bed shear stress, which can eventually become too low to suppress blooms of toxic cyanobacteria [*Power et al*., 2015] (K. Bouma-Gregson, personal communication, 2015). In this case, the potential for a bloom to occur depends on the persistence time, which, along with the total dry season length, determines the duration of the low flow period during which the bloom can develop.

In addition to these low-flow examples, high-flows can also initiate important ecological processes, for instance by submerging fish passage obstacles [*Reiser et al*., 2011; *Holmes et al*., 2015] and allowing migrations to extend into the upper reaches of watersheds; or by causing scouring of the stream bed. Taking the Eel River as an example again, observations suggest that bankfull flows mobilize enough sediment to dislodge or crush algae-grazing macroinvertebrates. This scour and associated loss of grazers promotes large dry season blooms of filamentous green algae, forming the structural backbone of dry season food webs that support salmonid fishes [*Power et al*., 2008]. The sequence of whether these thresholds are crossed or not during wet seasons and successive dry seasons can lead to substantially different ecological states [*Power et al*., 2015]. These situations should be readily amenable to stochastic analysis and incorporation into risk-based predictive frameworks.

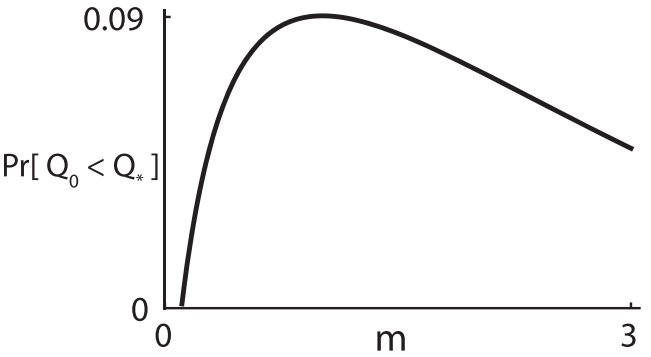

Figure 7. Probability that the dry season initial condition (Q_0) is less than a flow threshold set to 50% of the mean wet season flows for a range of realistic values of m.

5. Conclusion

This study developed a probabilistic model of the persistence time, T_{Q_*}, the number of days from the start of the dry season for which dry season flow exceeds Q_*. By linking the dry season recession to wet season flow dynamics through a dry season initial condition model (p_{Q_0}), the model analytically demonstrates the precise linkages between the dry season recession and simple measures of wet season hydroclimate and catchment geomorphology. In spite of excellent performance in the mean sense, the model did not incorporate an unexpected but essential source of variability: interannual fluctuations in the recession behavior, and correlation between the parameters used to describe it. The positive performance of the model overall suggests the potential for future work to exploit hydrologic predictions of the crossing properties of wet and dry season flows to support large-scale, rapid, in-stream ecological risk assessments. The challenges associated with capturing variability in seasonal recessions demonstrate the importance of improving understanding of recession variability. Parameter decorrelation emerges as a promising research avenue to separate the informative characteristics of hydrograph recessions from those that are purely attributable to the mathematical properties of the widely used power law model.

Appendix A: Resolving the Issue of Negative Persistence Times

It is possible that the dry season initial condition could be less than the flow threshold, ($Q_0 < Q_*$). In this case, the model will predict a negative persistence time. To resolve this issue, we discard years for which $Q_0 < Q_*$ and truncate all negative values in the persistence time PDF. For even reasonably high flow thresholds, this condition is true for only a small fraction of the years considered. With the flow threshold set at 50% of mean *wet season* flow $\left(\mathbb{E}[Q_w]=m/(2\gamma_Q)\right)$, which will be considerably higher than 50% of mean annual flow, this probability can be computed exactly using the cumulative distribution function of the dry season initial condition:

$$Pr[T_{Q_*} < 0]=Pr[Q_0 < Q_*]=P_{Q_0}\left[\frac{m}{2\gamma_Q}\right]=1-\frac{\Gamma\left(m+1,\frac{m}{2}\right)}{\Gamma(m+1)}. \tag{A1}$$

Figure 7 plots this probability across a broad range of realistic values for m. The maximum probability occurs for $m = 1$, and even in this case, $Q_0 < Q_*$ is expected to occur less than 10% of the time, even for this relatively high flow threshold. Therefore, discarding years with $Q_0 < Q_*$ will not significantly affect the quality of computed persistence time data.

Appendix B: Recession Parameter Correlation

The strong log-linear correlative relationship between the a and r parameters can be directly traced to the choice of a power law recession model: $\frac{dQ}{dt}=-aQ^{1-r}$ [*Bergner and Zouhar*, 2000]. This particular form of scale-dependent, artifactual correlation can be deliberately minimized through rescaling of the flow variable. *Bergner and Zouhar* [2000] analytically construct the scaling constant ($Q \rightarrow Q/Q_{scale}$):

$$Q_{scale}=10^{-\left(\frac{\sum_{i=1}^{n_j}(\bar{r}-r_i)_{\log(a_i/a_g)}}{\sum_{i=1}^{n_j}(\bar{r}-r_i)^2}\right)}, \tag{B1}$$

to force the linear correlation coefficient between $\log a$ and r to equal zero. Each Q_{scale} will be unique for a given catchment and is computed using the n_j fitted recession parameters, the mean of the r_i's ($\bar{r}$), and the geometric mean of the a_i's (a_g). Fitting recession curves to these new, rescaled recessions will yield a new set of n_j unique recession parameter pairs, $\left\{(\hat{a}_1,r_1),(\hat{a}_2,r_2),\ldots,(\hat{a}_{n_j},r_{n_j})\right\}$.

Acknowledgments
D. Dralle thanks the NSF GRFP. S.E. Thompson acknowledges support from NSF EAR-1331940. The authors would like to thank Suzanne Kelson from the Eel River Critical Zone Observatory for her images of Elder Creek, and Stephanie Carlson from the Environmental Science, Management, and Policy department at UC Berkeley for her edits and discussions regarding possible ecological applications of this work. All the streamflow data used for this study can be found on the website for United States Geological Survey (http://waterdata.usgs.gov/nwis).

References

Andermann, C., L. Longuevergne, S. Bonnet, A. Crave, P. Davy, and R. Gloaguen (2012), Impact of transient groundwater storage on the discharge of Himalayan rivers, *Nat. Geosci.*, *5*(2), 127–132, doi:10.1038/ngeo1356.

Annear, T. C., and A. L. Conder (1984), Relative bias of several fisheries instream flow methods, *N. Am. J. Fish. Manage.*, *4*, 531–539, doi:10.1577/1548-8659(1984)4<531:RBOSFI>2.0.CO;2.

Arnold, J. G., R. Srinivasan, R. S. Muttiah, and J. R. Williams (1998), Large area hydrologic modeling and assessment part i: Model development, *J. Am. Water Resour. Assoc.*, *34*(1), 73–89.

Bart, R., and A. Hope (2014), Inter-seasonal variability in baseflow recession rates: The role of aquifer antecedent storage in central California watersheds, *J. Hydrol.*, *519*, 205–213, doi:10.1016/j.jhydrol.2014.07.020.

Basso, S., M. Schirmer, and G. Botter (2015), On the emergence of heavy-tailed streamflow distributions, *Adv. Water Resour.*, *82*, 98–105.

Bergner, F., and G. Zouhar (2000), A new approach to the correlation between the coefficient and the exponent in the power law equation of fatigue crack growth, *Int. J. Fatigue*, *22*(3), 229–239.

Biswal, B., and M. Marani (2010), Geomorphological origin of recession curves, *Geophys. Res. Lett.*, *37*, L24403, doi:10.1029/2010GL045415.

Biswal, B., and M. Marani (2014), Universal' recession curves and their geomorphological interpretation, *Adv. Water Resour.*, *65*, 34–42, doi:10.1016/j.advwatres.2014.01.004.

Blöschl, G., M. Sivapalan, and T. Wagener (2013), *Runoff Prediction in Ungauged Basins: Synthesis Across Processes, Places and Scales*, Cambridge Univ. Press, Cambridge, England.

Botter, G., A. Porporato, I. Rodriguez-Iturbe, and A. Rinaldo (2007), Basin-scale soil moisture dynamics and the probabilistic characterization of carrier hydrologic flows: Slow, leaching-prone components of the hydrologic response, *Water Resour. Res.*, *43*, W02417, doi:10.1029/2006WR005043.

Botter, G., S. Zanardo, A. Porporato, I. Rodríguez-Iturbe, and A. Rinaldo (2008), Ecohydrological model of flow duration curves and annual minima, *Water Resour. Res.*, *44*, W08418, doi:10.1029/2008WR006814.

Botter, G., A. Porporato, I. Rodríguez-Iturbe, and A. Rinaldo (2009), Nonlinear storage-discharge relations and catchment streamflow regimes, *Water Resour. Res.*, *45*, W10427, doi:10.1029/2008WR007658.

Botter, G., S. Basso, I. Rodriguez-Iturbe, and A. Rinaldo (2013), Resilience of river flow regimes, *Proc. Natl. Acad. Sci. U. S. A.*, *110*(32), 12,925–12,930.

Brahmananda Rao, V., M. C. de Lima, and S. H. Franchito (1993), Seasonal and interannual variations of rainfall over eastern northeast Brazil, *J. Clim.*, *6*(9), 1754–1763, doi:10.1175/1520-0442(1993)006<1754:SAIVOR>2.0.CO;2.

Brutsaert, W., and J. L. Nieber (1977), Regionalized drought flow hydrographs from a mature glaciated plateau, *Water Resour. Res.*, *13*(3), 637–643, doi:10.1029/WR013i003p00637.

Castellarin, A., G. Galeati, L. Brandimarte, A. Montanari, and A. Brath (2004), Regional flow-duration curves: Reliability for ungauged basins, *Adv. Water Resour.*, *27*(10), 953–965.

Castellarin, A., G. Camorani, and A. Brath (2007), Predicting annual and long-term flow-duration curves in ungauged basins, *Adv. Water Resour.*, *30*(4), 937–953.

CIESIN (2012), *National Aggregates of Geospatial Data Collection: Population, Landscape, And Climate Estimates*, Version 3 (PLACE III), NASA, Socioecon. Data and Appl. Cent., N. Y., doi:10.7927/H4F769GP.

Cortie, M. B. (1991), The irrepressable relationship between the Paris law parameters, *Eng. Fract. Mech.*, *40*(3), 681–682, doi:10.1016/0013-7944(91)90160-3.

D'odorico, P., L. Ridolfi, A. Porporato, and I. Rodriguez-Iturbe (2000), Preferential states of seasonal soil moisture: The impact of climate fluctuations, *Water Resour. Res.*, *36*(8), 2209–2219, doi:10.1029/2000WR900103.

Dominguez, F., E. Rivera, D. P. Lettenmaier, and C. L. Castro (2012), Changes in winter precipitation extremes for the western United States under a warmer climate as simulated by regional climate models, *Geophys. Res. Lett.*, *39*, L05803, doi:10.1029/2011GL050762.

Doulatyari, B., S. Basso, M. Schirmer, and G. Botter (2014), River flow regimes and vegetation dynamics along a river transect, *Adv. Water Resour.*, *73*, 30–43, doi:10.1016/j.advwatres.2014.06.015.

Fatichi, S., V. Y. Ivanov, and E. Caporali (2012), Investigating interannual variability of precipitation at the global scale: Is there a connection with seasonality?, *J. Clim.*, *25*(16), 5512–5523, doi:10.1175/JCLI-D-11-00356.1.

Feng, X., G. Vico, and A. Porporato (2012), On the effects of seasonality on soil water balance and plant growth, *Water Resour. Res.*, *48*, W05543, doi:10.1029/2011WR011263.

Feng, X., A. Porporato, and I. Rodríguez-Iturbe (2015), Stochastic soil water balance under seasonal climates, *Proc. R. Soc. A*, *471*(2174), doi:10.1098/rspa.2014.0623.

Fullerton, A. H., K. M. Burnett, E. A. Steel, R. L. Flitcroft, G. R. Pess, B. E. Feist, C. E. Togersen, D. J. Miller, and B. L. Sanderson (2010), Hydrological connectivity for riverine fish: Measurement challenges and research opportunities, *Freshwater Biol.*, *55*(11), 2215–2237, doi:10.1111/j.1365-2427.2010.02448.x.

Ganora, D., P. Claps, F. Laio, and A. Viglione (2009), An approach to estimate nonparametric flow duration curves in ungauged basins, *Water Resour. Res.*, *45*, W10418, doi:10.1029/2008WR007472.

Gao, X., and F. Giorgi (2008), Increased aridity in the Mediterranean region under greenhouse gas forcing estimated from high resolution simulations with a regional climate model, *Global Planet. Change*, *62*(3–4), 195–209, doi:10.1016/j.gloplacha.2008.02.002.

García-Ruiz, J. M., J. I. López-Moreno, S. M. Vicente-Serrano, T. Lasanta Martínez, and S. Beguería (2011), Mediterranean water resources in a global change scenario, *Earth Sci. Rev.*, *105*(3–4), 121–139, doi:10.1016/j.earscirev.2011.01.006.

Harman, C. J., M. Sivapalan, and P. Kumar (2009), Power law catchment-scale recessions arising from heterogeneous linear small-scale dynamics, *Water Resour. Res.*, *45*, W09404, doi:10.1029/2008WR007392.

Holmes, R. W., D. E. Rankin, E. Ballard, and M. Gard (2015), Evaluation of Steelhead passage flows using hydraulic modeling on an unregulated coastal California River, *River Res. Appl.*, doi:10.1002/rra.2884, in press.

Hussain, M. A., S. Kar, and R. R. Puniyani (1999), Relationship between power law coefficients and major blood constituents affecting the whole blood viscosity, *J. Biosci.*, *24*(3), 329–337, doi:10.1007/BF02941247.

Hwan, J. L., and S. M. Carlson (2015), Fragmentation of an intermittent stream during seasonal drought: Intra-annual and interannual patterns and biological consequences, *River Res. Appl.*, doi:10.1002/rra.2907, in press.

Kirchner, J. W. (2009), Catchments as simple dynamical systems: Catchment characterization, rainfall-runoff modeling, and doing hydrology backward, *Water Resour. Res.*, *45*, W02429, doi:10.1029/2008WR006912.

Klausmeyer, K. R., and M. R. Shaw (2009), Climate change, habitat loss, protected areas and the climate adaptation potential of species in mediterranean ecosystems worldwide, *PLoS One*, *4*, doi:10.1371/journal.pone.0006392.

Krueger, T., J. Freer, J. N. Quinton, C. J. A. Macleod, G. S. Bilotta, R. E. Brazier, P. Butler, and P. M. Haygarth (2010), Ensemble evaluation of hydrological model hypotheses, *Water Resour. Res.*, *46*, W07516, doi:10.1029/2009WR007845.
Kumagai, T., N. Yoshifuji, and N. Tanaka (2009), Comparison of soil moisture dynamics between a tropical rain forest and a tropical seasonal forest in southeast Asia: Impact of seasonal and year-to-year variations in rainfall, *Water Resour. Res.*, *45*, W04413, doi:10.1029/2008WR007307.
Laaha, G., and G. Blöschl (2007), A national low flow estimation procedure for Austria, *Hydrol. Sci. J.*, *52*(4), 625–644.
Laio, F. (2002), On the seasonal dynamics of mean soil moisture, *J. Geophys. Res.*, *107*(D15), 4272, doi:10.1029/2001JD001252.
Laio, F., A. Porporato, L. Ridolfi, and I. Rodriguez-Iturbe (2001), Mean first passage times of processes driven by white shot noise, *Phys. Rev. E*, *63*(3), 036105, doi:10.1103/PhysRevE.63.036105.
Mather, A. L., and R. L. Johnson (2014), Quantitative characterization of stream turbidity-discharge behavior using event loop shape modeling and power law parameter decorrelation, *Water Resour. Res.*, *50*, 7766–7779, doi:10.1016/S0142-1123(99)00123-1.
McMillan, H., M. Gueguen, E. Grimon, R. Woods, M. Clark, and D. E. Rupp (2014), Spatial variability of hydrological processes and model structure diagnostics in a 50km^2 catchment, *Hydrol. Processes*, *28*(18), 4896–4913, doi:10.1002/hyp.9988.
Miles, L., A. C. Newton, R. S. DeFries, C. Ravilious, I. May, S. Blyth, V. Kapos, and J. E. Gordon (2006), A global overview of the conservation status of tropical dry forests, *J. Biogeogr.*, *33*(3), 491–505, doi:10.1111/j.1365-2699.2005.01424.x.
Miller, G. R., D. D. Baldocchi, B. E. Law, and T. Meyers (2007), An analysis of soil moisture dynamics using multi-year data from a network of micrometeorological observation sites, *Adv. Water Resour.*, *30*, 1065–1081, doi:10.1016/j.advwatres.2006.10.002.
Milly, P. C. D. (1993), An analytic solution of the stochastic storage problem applicable to soil water, *Water Resour. Res.*, *29*(11), 3755–3758, doi:10.1029/93WR01934.
Moore, R. D. (1997), Storage-outflow modelling of streamflow recessions, with application to a shallow-soil forested catchment, *J. Hydrol.*, *198*, 260–270, doi:10.1016/S0022-1694(96)03287-8.
Müller, M. F., and S. E. Thompson (2015), A topological restricted maximum likelihood (TopREML) approach to regionalize trended runoff signatures in stream networks, *Hydrol. Earth Syst. Sci. Discuss.*, *12*(1), 1355–1396, doi:10.5194/hessd-12-1355-2015.
Müller, M. F., D. N. Dralle, and S. E. Thompson (2014), Analytical model for flow duration curves in seasonally dry climates, *Water Resour. Res.*, *50*, 5510–5531, doi:10.1002/2014WR015301.
Nash, J. E., and J. V. Sutcliffe (1970), River flow forecasting through conceptual models part I: A discussion of principles, *J. Hydrol.*, *10*(3), 282–290, doi:10.1016/0022-1694(70) 90255-6.
Nathan, R. J., and T. A. McMahon (1992), Estimating low flow characteristics in ungauged catchments, *Water Resour. Manage.*, *6*(2), 85–100.
Nelson, F. A. (1980), Evaluation of Four Instream Flow Methods Applied to Four Trout Rivers in Southwest Montana, Mont. Dep. of Fish Wildlife and Parks, Helena, Montana, doi:10.5962/bhl.title. 23324.
Nielsen, J. L., T. E. Lisle, and V. Ozaki (1994), Thermally stratified pools and their use by steelhead in northern California streams, *Trans. Am. Fish. Soc.*, *123*, 613–626, doi:10.1577/1548-8659(1994)123<0613:TSPATU>2.3.CO;2.
Parker, G. W., and D. S. Armstrong (2001), Preliminary assessment of streamflow requirements for habitat protection for selected sites on the Assabet and Charles Rivers, eastern Massachusetts, *U.S. Geol. Surv. Open-File Rep., 02-340*, 35 p.
Patnaik, S., B. Biswal, D. N. Kumar, and B. Sivakumar (2015), Effect of catchment characteristics on the relationship between past discharge and the power law recession coefficient, *J. Hydrol.*, *528*, 321–328.
Peel, M. C., and B. L. Finlayson (2007), Updated world map of the Köppen-Geiger climate classification, *Hydrol. Earth Syst. Sci.*, *4*, 439–473, doi:10.5194/hess-11-1633-2007.
Porporato, A., F. Laio, L. Ridolfi, and I. Rodriguez-Iturbe (2001), Plants in water-controlled ecosystems: Active role in hydrologic processes and response to water stress: III. Vegetation water stress, *Adv. Water Resour.*, *24*(7), 725–744, doi:10.1016/S0309-1708(01)00006-9.
Porporato, A., E. Daly, and I. Rodríguez-Iturbe (2004), Soil water balance and ecosystem response to climate change, *Am. Nat.*, *164*(5), 625–632, doi:10.1086/424970.
Power, M. E., M. S. Parker, and W. E. Dietrich (2008), Seasonal reassembly of a river food web: Floods, droughts, and impacts of fish, *Ecol. Monogr.*, *78*(2), 263–282, doi:10.1890/06-0902.1.
Power, M. E., K. Bouma-Gregson, P. Higgins, and S. M. Carlson (2015), The thirsty eel: Summer and winter flow thresholds that tilt the eel river of northwestern California from salmon-supporting to cyanobacterially degraded states, *Copeia*, *2015*(1), 200–211, doi:10.1643/CE-14-086.
Reiser, D. W., C. Huang, S. Beck, M. Gagner, and E. Jeanes (2011), Defining flow windows for upstream passage of adult anadromous salmonids at Cascades and Falls, *Trans. Am. Fish. Soc.*, *135*(3), 668–679, doi:10.1577/T05-169.1.
Rodriguez-Iturbe, I., A. Porporato, L. Ridolfi, V. Isham, and D. R. Coxi (1999), Probabilistic modelling of water balance at a point: The role of climate, soil and vegetation, *Proc. R. Soc. A*, *455*(1990), 3789–3805, doi:10.1098/rspa.1999.0477.
Samuel, J. M., M. Sivapalan, and I. Struthers (2008), Diagnostic analysis of water balance variability: A comparative modeling study of catchments in Perth, Newcastle, and Darwin, Australia, *Water Resour. Res.*, *44*, W06403, doi:10.1029/2007WR006694.
Sawaske, S. R., and D. L. Freyberg (2014), An analysis of trends in baseflow recession and low-flows in rain-dominated coastal streams of the pacific coast, *J. Hydrol.*, *519*, 599–610.
Shaw, S. B., and S. J. Riha (2012), Examining individual recession events instead of a data cloud: Using a modified interpretation of dQ/dt–Q streamflow recession in glaciated watersheds to better inform models of low flow, *J. Hydrol.*, *434-435*, 46–54, doi:10.1016/j.jhydrol.2012.02.034.
Shih, W., M. Orlowski, and K. Y. Fu (1990), Parameter correlation and modeling of the power-law relationship in mosfet hot-carrier degradation, *IEEE Elect. Device Lett.*, *11*(7), 297–299, doi:10.1109/55.56480.
Skøien, J. O., R. Merz, and G. Blöschl (2006), Top-kriging-geostatistics on stream networks, *Hydrol. Earth Syst. Sci.*, *10*(2), 277–287.
Szilagyi, J., M. B. Parlange, and J. D. Albertson (1998), Recession flow analysis for aquifer parameter determination, *Water Resour. Res.*, *34*(7), 1851–1857, doi:10.1029/98WR01009.
Tague, C., and G. E. Grant (2004), A geological framework for interpreting the low-flow regimes of Cascade streams, Willamette River Basin, Oregon, *Water Resour. Res.*, *40*, W04303, doi:10.1029/2003WR002629.
Tamea, S., F. Laio, L. Ridolfi, and I. Rodriguez-Iturbe (2011), Crossing properties for geophysical systems forced by Poisson noise, *Geophys. Res. Lett.*, *38*, L18404, doi:10.1029/2011GL049074.
Thompson, K. (1972), *Determining stream flows for fish life*, Pacific Northwest River Basins Commission, In *stream Flow Requirement Workshop*, The Commission, Portland, Oreg.
Thompson, S., S. Levin, and I. Rodríguez-Iturbe (2013), Linking plant disease risk and precipitation drivers: A dynamical systems framework, *Am. Nat.*, *181*(1), E1–E16, doi:10.1086/668572.
Thompson, S. E., S. Levin, and I. Rodríguez-Iturbe (2014), Rainfall and temperatures changes have confounding impacts on Phytophthora cinnamomi occurrence risk in the southwestern USA under climate change scenarios, *Global Change Biol.*, *20*(4), 1299–1312, doi:10.1111/gcb.12463.

Turner, L., and W. D. Erskine (2005), Variability in the development, persistence and breakdown of thermal, oxygen and salt stratification on regulated rivers of Southeastern Australia, *River Res. Appl.*, *21*, 151–168, doi:10.1002/rra.838.

Underwood, E. C., J. H. Viers, K. R. Klausmeyer, R. L. Cox, and M. R. Shaw (2009), Threats and biodiversity in the mediterranean biome, *Divers. Distrib.*, *15*(2), 188–197, doi:10.1111/j.1472-4642.2008.00518.x.

Vico, G., et al. (2014), Climatic, ecophysiological, and phenological controls on plant ecohydrological strategies in seasonally dry ecosystems, *Ecohydrology*, *8*, 660–681, doi:10.1002/eco.1533.

Viola, F., E. Daly, G. Vico, M. Cannarozzo, and A. Porporato (2008), Transient soil-moisture dynamics and climate change in mediterranean ecosystems, *Water Resour. Res.*, *44*, W11412, doi:10.1029/2007WR006371.

Zilberstein, V. A. (1992), On correlations between the power law parameters, *Int. J. Fract.*, *58*(3), R57–R59, doi:10.1007/BF00015624.